Improving Attitude Estimation Using Inertial Sensors for Quadrotor Control Systems*

Ricardo Sanz, Luis Ródenas and Pedro García
Instituto de Automática e Informática Industrial
Universidad Politécnica de Valencia
Valencia, 46022 Spain
{*rsanz,luirdelo,pggil*}*@aii.upv.es*

Pedro Castillo
LAFMIA UMI 3175
CINVESTAV - CNRS
Mexico
castillo@hds.utc.fr

***Abstract*— Attitude estimation for an aerial vehicle using the Kalman Filter - KF- with experimental validation is presented in this paper. The data fusion is made using simplified representations of the kinematics of the aerial vehicle and the accelerometer measurement model. The resulting algorithm is computationally efficient as it can be run at up to 500 Hz on a low-cost microcontroller. The observer is improved by choosing the appropriate covariance and noise matrices. Numerical and in-flight validation are carried out using two prototypes and the experimental results are compared online with the measure coming from a commercial IMU -Inertial Measurement Unit.**

***Index Terms*— Attitude estimation, observers, real-time validation, EKF**

I. Introduction

Unmanned Aircraft Systems (UAS) are systems whose components include the necessary equipment, network, and personnel to control an unmanned aircraft. Growth in unmanned platforms of all sizes and shapes has been substantial, with a corresponding increase in payload numbers and capability. Several of these systems were developed using the deliberative requirements and acquisitions processes.

The pace of technological advances across the broad spectrum of unmanned systems applications has allowed what were once rather cumbersome vehicles and systems outside the ”circle of civil applications” to shoulder tasks in civil mission areas only a few years ago. Nowadays it is possible to use UAS for civil purposes like ground traffic inspection [1], forest fire monitoring [2] or real-time irrigation control [3].

With dramatic increases in battery life and computer processing; reduction in size and complexity of sensors; and improvements in reliability, maintainability, automation, and operator interfaces, unmanned systems are now vital components of a civil applications tool kit [4].

When it comes to civil applications, reducing the cost of the UAS to a minimum is a must. Inertial Measurement Units (IMUs), which are the core of lightweight robotic vehicles usually represent a large portion of their total cost [5]. These devices provide an estimation of the vehicle attitude by fusing measurements coming from accelerometers, gyroscopes and magnetometers.

There are several approaches to solve the attitude estimation problem. Despite the lack of convergence and optimality guarantees, the Extended Kalman Filter (EKF) has been the workhorse of real-time spacecraft attitude estimation for quite some time [6]. The earliest published application was [7] in 1970 by Farrell and several others have followed since. Lefferts, Shuster, and Markley published a thorough review of the topic [8] in 1982 and since then Markley, Crassidis, and several others have kept Kalman filtering an active topic of research in the space industry [9]–[11]. Several different attitude representations have been used in Kalman filtering with varying degrees of success.

In this paper, a computationally efficient algorithm to estimate the attitude of a rotorcraft is proposed and validated in flight tests. The approach consists of a Kalman filter applied to the kinematics of the vehicle represented by means of the Euler formulation, and including the biases of the gyroscopes into the vector of estimated variables. In addition, the experimental results are compared with the data coming from a commercial IMU showing the good behavior of the estimation algorithm. The methodology followed in this paper is similar to that of [12]. However, in contrast to the method proposed in this paper, the work in [12] does not estimate the biases of the gyroscopes, which can lead to important errors after several minutes of operation.

The paper is structured as follows. Basis and notation to introduce the main concepts are described in section II. The attitude estimation algorithm is explained in section III. Numerical validation results in a fixed-platform are presented in Section IV, while flight tests are analyzed and described in Section V. Finally, some discussions about this work are presented in section VI.

II. Basis and notation

The basis for analysis, computation or simulation of the unsteady motions of a flight vehicle is the mathematical model of the vehicle and its subsystems. The velocities and

*This work has been partially supported by; PROMETEO project No. 2008-088, Consellería de Educación GV, Universidad Politécnica de Valencia PAID-06-12 and CICYT Project DPI2011-28507-C02-01, Spain.

accelerations must of course be relative to an inertial, or Newtonian, frame of reference.

Thus, let us denote by $\{\hat{\boldsymbol{e}}_1, \hat{\boldsymbol{e}}_2, \hat{\boldsymbol{e}}_3\}$ the unit basis vectors of the Earth-Centered Earth-fixed (ECEF) reference frame, $\{E\}$, which is assumed to be inertial.

Let $\boldsymbol{\omega} = \boldsymbol{\omega}^B_{B/E} = [p, q, r]^T$ be the angular velocity of the aircraft with respect to $\{E\}$ expressed in the body frame $\{B\}$. The rotational kinematic relating these angular velocities to the Euler angles, $\boldsymbol{\eta} = [\phi\, \theta\, \psi]^T$, is expressed as

$$\dot{\boldsymbol{\eta}} = \begin{bmatrix} 1 & \sin\phi\tan\theta & \cos\phi\tan\theta \\ 0 & \cos\phi & -\sin\phi \\ 0 & \frac{\sin\phi}{\cos\theta} & \frac{\cos\phi}{\cos\theta} \end{bmatrix} \boldsymbol{\omega} \tag{1}$$

where ϕ, θ, and ψ denote the roll, pitch and yaw angle, respectively.

The orientation of $\{B\}$ with respect to $\{E\}$ is represented by means of the rotation matrix, ${}^{\mathrm{B}}\boldsymbol{R}_E$, which can be expressed in terms of the Euler angles as

$${}^{\mathrm{B}}\boldsymbol{R}_E = \begin{bmatrix} c\theta c\psi & c\theta s\psi & -s\theta \\ s\phi s\theta c\psi - c\phi s\psi & s\phi s\theta s\psi + c\phi c\psi & s\phi c\theta \\ c\phi s\theta c\psi + s\phi s\psi & c\phi s\theta s\psi - c\phi c\psi & c\phi s\theta \end{bmatrix} \tag{2}$$

using the conventional sequence of roll-pitch-yaw.

Notice that the representation in (2) has a singularity at $\theta = 180°$. A quaternion-based representation can solve this inconvenient, however, the civil missions usually do not require to perform acrobatic maneuvers. Therefore, Euler angles are valid for these purposes. In addition, the estimation will be restricted to the roll and pitch angles, as they are responsible for keeping the aerial vehicle at hover. Hence the yaw angle is not considered for this work.

It is important to express in a mathematical form the relation between the external forces acting on the vehicle with the accelerations and angular rate measurements coming from the inertial sensors. Notice that, the accelerometers in strap-down configuration measure the specific force acting on the vehicle expressed in $\{B\}$ as they are aligned with the body-fixed reference frame. Thus without loss of generality, the measurement can be expressed as

$$\boldsymbol{a}^B = \frac{1}{m}\left(\boldsymbol{f}^B - {}^{\mathrm{B}}\boldsymbol{R}_E(mg)\hat{\boldsymbol{e}}_3\right) = \dot{\boldsymbol{v}}^B - {}^{\mathrm{B}}\boldsymbol{R}_E g\hat{\boldsymbol{e}}_3 \tag{3}$$

where $\dot{\boldsymbol{v}}^B$ is the acceleration vector due to the external forces expressed in $\{B\}$, m denotes the mass of the aerial vehicle and $\boldsymbol{f}^B$ represents the vector of external forces that act on the quadrotor. Since the accelerations in stable flight regimes are usually small compared to the gravity acceleration, neglecting the linear acceleration ($\dot{\boldsymbol{v}}^B = 0$) is a classical assumption [13]. Normalizing the vector of acceleration measurements facilitates to express the roll and pitch angles as

$$\boldsymbol{a} = \frac{\boldsymbol{a}^B}{|\boldsymbol{a}^B|} \approx -{}^{\mathrm{B}}\boldsymbol{R}_E\hat{\boldsymbol{e}}_3 = \begin{bmatrix} \sin\theta \\ -\sin\phi\cos\theta \\ -\cos\phi\cos\theta \end{bmatrix} \tag{4}$$

Let us consider the following model for the inertial sensors,

$$\begin{aligned} \bar{\boldsymbol{\omega}} &= \boldsymbol{\omega} + \boldsymbol{\beta}_\omega + \boldsymbol{\eta}_\omega \\ \bar{\boldsymbol{a}} &= \mathbf{a} + \boldsymbol{\eta}_a \end{aligned} \tag{5}$$

where the velocity measurement $\bar{\boldsymbol{\omega}}$ is composed of its actual value $\boldsymbol{\omega}$, plus the bias $\boldsymbol{\beta}_\omega$ and noise in the measurement $\boldsymbol{\eta}_\omega$. The same applies for the acceleration measurement but the biases are not included. These errors are not so critical as they are not integrated over time. The measurement noises are subject to a Gaussian representation as follows,

$$\begin{aligned} \mathbb{E}[\boldsymbol{\eta}_\omega] = 0 \qquad & \mathbb{E}[\boldsymbol{\eta}_\omega\boldsymbol{\eta}_\omega^T] = \boldsymbol{\Sigma}_\omega = \sigma_\omega^2\boldsymbol{I}_3 \\ \mathbb{E}[\boldsymbol{\eta}_a] = 0 \qquad & \mathbb{E}[\boldsymbol{\eta}_a\boldsymbol{\eta}_a^T] = \boldsymbol{\Sigma}_a = \sigma_a^2\boldsymbol{I}_3 \end{aligned} \tag{6}$$

where $\boldsymbol{\Sigma}_\omega$ and $\boldsymbol{\Sigma}_a$ define the diagonal covariance matrices.

The following random walk process,

$$\dot{\boldsymbol{\beta}}_\omega = \boldsymbol{\eta}_\beta, \tag{7}$$

$$\mathbb{E}[\boldsymbol{\eta}_\beta] = 0, \qquad \mathbb{E}[\boldsymbol{\eta}_\beta\boldsymbol{\eta}_\beta^T] = \boldsymbol{\Sigma}_\beta = \sigma_\beta^2\boldsymbol{I}_3, \tag{8}$$

is used to model the "slowly-varying" biases of the gyros, where $\boldsymbol{\eta}_\beta$ is white noise and $\boldsymbol{\Sigma}_\beta$ is its diagonal covariance matrix. The variance σ_β^2 determines how much the bias drifts.

Recall that the Kalman filter is derived for a system described by

$$\begin{aligned} \dot{\boldsymbol{x}} &= \boldsymbol{A}\boldsymbol{x} + \boldsymbol{w} \qquad & \mathbb{E}[\boldsymbol{w}\boldsymbol{w}^T] &= \boldsymbol{Q} \\ \boldsymbol{y} &= \boldsymbol{C}\boldsymbol{x} + \boldsymbol{v} \qquad & \mathbb{E}[\boldsymbol{v}\boldsymbol{v}^T] &= \boldsymbol{R} \end{aligned} \tag{9}$$

where $\boldsymbol{w}$ and $\boldsymbol{v}$ are the process and the measurement noises, respectively, which are assumed to be Gaussian, with covariance matrices $\boldsymbol{Q}$ and $\boldsymbol{R}$. Observe that, it is thus necessary to estimate and correct the biases of the sensors as they are nearly constant errors which are not removed in the Kalman filtering process. Moreover, it is convenient to identify the stochastic model of the sensors for achieving a good performance.

III. Proposed algorithm

The kinematics of an aerial vehicle and the measurement model can be expressed by (1) and (4), respectively. An advantage of the Euler formulation is that the yaw angle can be removed from the equations. Let us denote the state vector of estimated variables by $\boldsymbol{x} = [\phi,\, \beta_x,\, \theta,\, \beta_y]$. Thus, the filter can be written as

$$\begin{aligned} \dot{\boldsymbol{x}} &= \begin{bmatrix} (\bar{\omega}_x - \beta_x) + (\bar{\omega}_y - \beta_y)\sin\phi\tan\theta \\ 0 \\ (\bar{\omega}_y - \beta_y)\cos\phi \\ 0 \end{bmatrix} + \boldsymbol{w} \\ \boldsymbol{y} &= \begin{bmatrix} \sin\theta \\ -\sin\phi\cos\theta \\ -\cos\phi\cos\theta \end{bmatrix} + \boldsymbol{v} \end{aligned} \tag{10}$$

Moreover, it is reasonable to simplify the equations by assuming small angles approximations, $\sin\alpha \approx \alpha$ and $\cos\alpha \approx 1$,

with $\alpha = \{\phi,\, \theta\}$, which leads to the following linear equations

$$\begin{aligned}\dot{\boldsymbol{x}} &= \begin{bmatrix}0 & -1 & 0 & 0\\ 0 & 0 & 0 & 0\\ 0 & 0 & 0 & -1\\ 0 & 0 & 0 & 0\end{bmatrix}\boldsymbol{x} + \begin{bmatrix}1 & 0\\ 0 & 0\\ 0 & 1\\ 0 & 0\end{bmatrix}\boldsymbol{u} + \boldsymbol{w}\\ \boldsymbol{y} &= \begin{bmatrix}0 & 0 & 1 & 0\\ -1 & 0 & 0 & 0\end{bmatrix}\boldsymbol{v} + \boldsymbol{v}\end{aligned} \tag{11}$$

where the input vector consists of the angular velocity measurements $\boldsymbol{u} = [\bar{\omega}_x,\, \bar{\omega}_y]$, and $\boldsymbol{y} = [\bar{a}_x,\, \bar{a}_y]$ contains the acceleration measurements. The third equation of the measurement model which involves the third accelerometer axis has been removed, as it has very low sensitivity with respect to the roll-pitch orientation for small angles.

These simplifications result in a smaller-size linear system thus reducing the computational load substantially. Furthermore, it will be shown next how the structure of the matrices can be also exploited to reduce the Kalman filter to a set of simple equations. The continuous-time system (11) can be discretized with sample time T, assuming zero-order hold of the input, as follows

$$\begin{aligned}\boldsymbol{x}_{k+1} &= \boldsymbol{A}_k\boldsymbol{x}_k + \boldsymbol{B}_k\boldsymbol{u}_k + \boldsymbol{w}_k & \mathbb{E}[\boldsymbol{w}_k\boldsymbol{w}_k^T] &= \boldsymbol{Q}_k\\ \boldsymbol{y}_k &= \boldsymbol{H}_k\boldsymbol{x}_k + \boldsymbol{v}_k & \mathbb{E}[\boldsymbol{v}_k\boldsymbol{v}_k^T] &= \boldsymbol{R}_k\end{aligned} \tag{12}$$

where

$$\begin{aligned}\boldsymbol{A}_k &= e^{\boldsymbol{A}T} = \begin{bmatrix}1 & -T & 0 & 0\\ 0 & 1 & 0 & 0\\ 0 & 0 & 1 & -T\\ 0 & 0 & 0 & 1\end{bmatrix}\\ \boldsymbol{B}_k &= \int_0^T e^{\boldsymbol{A}\tau}\mathrm{d}\tau = \begin{bmatrix}T & 0\\ 0 & 0\\ 0 & T\\ 0 & 0\end{bmatrix}\\ \boldsymbol{H}_k &= \begin{bmatrix}0 & 0 & 1 & 0\\ -1 & 0 & 0 & 0\end{bmatrix}\end{aligned}$$

Notice that, as a consequence of the simplifications, the resulting system is decoupled. Therefore, one can implement two different Kalman filters separately for roll and pitch. The equations of the EKF can be found in [14] and are summarized as

$$\begin{aligned}\boldsymbol{x}_k^- &= \boldsymbol{A}_{k-1}\boldsymbol{x}_{k-1} + \boldsymbol{B}_{k-1}\boldsymbol{u}_{k-1}\\ \boldsymbol{P}_k^- &= \boldsymbol{A}_{k-1}\boldsymbol{P}_{k-1}\boldsymbol{A}_{k-1}^T + \boldsymbol{Q}_k\end{aligned} \tag{13}$$

$$\begin{aligned}\boldsymbol{S}_k &= \boldsymbol{H}_k\boldsymbol{P}_k^-\boldsymbol{H}_k^T + \boldsymbol{R}_k\\ \boldsymbol{K}_k &= \boldsymbol{P}_k^-\boldsymbol{H}_h^T\boldsymbol{S}_k^{-1}\\ \boldsymbol{x}_k^+ &= \boldsymbol{x}_k^- + \boldsymbol{K}_k\left(\boldsymbol{y}_k - \boldsymbol{H}_k\boldsymbol{x}_k^-\right)\\ \boldsymbol{P}_k^+ &= (\boldsymbol{I} - \boldsymbol{K}_k\boldsymbol{H}_k)\boldsymbol{P}_k^-\end{aligned} \tag{14}$$

One can take advantage of the fact that the matrix $\boldsymbol{P}$ is symmetric, so that only three of its entries need to be stored in memory. Using (13) and (14), the following equations for the Kalman filter of the roll angle can be derived

$$\begin{aligned}\phi_k^- &= \phi_{k-1} + T(\bar{\omega}_x - \beta_{x_k})\\ \beta_{x_k}^- &= \beta_{x_{k-1}}\\ p_{11_k}^- &= p_{11_{k-1}} - 2Tp_{12_{k-1}} + T^2p_{22_{k-1}} + q_{11_k}\\ p_{12_k}^- &= p_{12_{k-1}} - Tp_{22_{k-1}}\\ p_{22_k}^- &= p_{22_{k-1}} + q_{22_k}\end{aligned} \tag{15}$$

$$\begin{aligned}\phi_k^+ &= (1-\alpha_\phi)\phi_k^- - \alpha_\phi\bar{a}_y\\ \beta_{x_k}^+ &= \beta_{x_k}^- - \gamma_\phi(\bar{a}_y + \phi_k^-)\\ p_{11_k}^+ &= (1-\alpha_\phi)p_{11_k}^-\\ p_{12_k}^+ &= (1-\alpha_\phi)p_{12_k}^-\\ p_{22_k}^+ &= -\gamma_\phi p_{12_k}^- + p_{22_k}^-\end{aligned} \tag{16}$$

where

$$\alpha_\phi = \frac{p_{11_k}^+}{p_{11_k}^+ + r_{11}} \qquad \gamma_\phi = \frac{p_{12_k}^+}{p_{11_k}^+ + r_{11_k}} \tag{17}$$

In a very similar way, the derivation of the Kalman filter equations for the pitch angle leads to the following set of equations

$$\begin{aligned}\theta_k^- &= \theta_{k-1} + T(\bar{\omega}_x - \beta_{x_k})\\ \beta_{y_k}^- &= \beta_{y_{k-1}}\\ p_{11_k}^- &= p_{11_{k-1}} - 2Tp_{12_{k-1}} + T^2p_{22_{k-1}} + q_{33_k}\\ p_{12_k}^- &= p_{12_{k-1}} - Tp_{22_{k-1}}\\ p_{22_k}^- &= p_{22_{k-1}} + q_{44_k}\end{aligned} \tag{18}$$

$$\begin{aligned}\theta_k^+ &= (1-\alpha_\phi)\theta_k^- + \alpha_\phi\bar{a}_y\\ \beta_{y_k}^+ &= \beta_{y_k}^- + \gamma_\phi(\bar{a}_x - \theta_k^-)\\ p_{11_k}^+ &= (1-\alpha_\theta)p_{11_k}^-\\ p_{12_k}^+ &= (1-\alpha_\theta)p_{12_k}^-\\ p_{22_k}^+ &= -\gamma_\theta p_{12_k}^- + p_{22_k}^-\end{aligned} \tag{19}$$

where

$$\alpha_\theta = \frac{p_{11_k}^+}{p_{11_k}^+ + r_{22_k}} \qquad \gamma_\theta = \frac{p_{12_k}^+}{p_{11_k}^+ + r_{22_k}} \tag{20}$$

IV. Numerical validation

The Kalman filter algorithm proposed for attitude estimation has been first validated using the platform shown in Fig. 1. It is thought of as a test bed platform of control algorithms for vertical lift off vehicles, so that the translational degrees of freedom are clamped for convenience.

The orientation of the vehicle is measured by means of optical encoders with an accuracy of 0.04 deg. These encoders provide a reliable pattern for the evaluation and comparison of the algorithms. In addition, a commercial IMU (3DM-GX2) and a low cost inertial sensor (MPU6050) were also included in the platform in order to validate and compare the

measurements. The 3DM-GX2 runs at 200 Hz and outputs directly the orientation in Euler angles representation. The MPU6050 is composed of a 3-axis gyroscope and a 3-axis accelerometer. It does not provide the angles of the rigid body but only the raw measurements of the sensors. The characteristics of the both devices are given in table I.

TABLE I

IMUS SPECIFICATIONS

	Microstrain 3DM-GX2	MPU-6050
Size	$63 \times 41 \times 32$	$21 \times 17 \times 2$
Weight	50 g	6 g
Gyro range	± 75 to ± 1200 deg/s	± 250 to ± 2000 deg/s
Gyro bias	± 0.2 deg/s	± 20 deg/s
Gyro nonlinearity	0.2 %	0.2%
Gyro noise performance	0.17 deg/s (rms) [a]	0.025 deg/s/ (rms)
Accel. bias	± 5 mg	± 50 mg
Accel. nonlinearity	0.2 %	0.5 %
Accel. noise performance	0.6 mg (rms) [a]	1.3 mg (rms)

[a] Measured from static output of the sensor

A PD controller was used to stabilize the system to constant references of pitch and roll. The system was then perturbed applying disturbances by hand. All data was collected at 333 Hz and the algorithm described in Section III was computed offline using Matlab. A trial and error tuning process resulted in the following covariance matrices

$$\boldsymbol{Q}_k = \begin{bmatrix} 0.94 \cdot 10^{-6} & 0 & 0 & 0 \\ 0 & 0.91 \cdot 10^{-6} & 0 & 0 \\ 0 & 0 & 0 & 0 \\ 0 & 0 & 0 & 0 \end{bmatrix}$$

$$\boldsymbol{R}_k = \begin{bmatrix} 0.37 & 0 \\ 0 & 0.39 \end{bmatrix}$$

The estimation obtained by means of this procedure can be seen in Fig. 2. At first sight, it can be noticed that the proposed algorithm performs fairly well, thus validating the simplifications made on its derivation. As it is difficult to visually evaluate the quality of both estimations, some

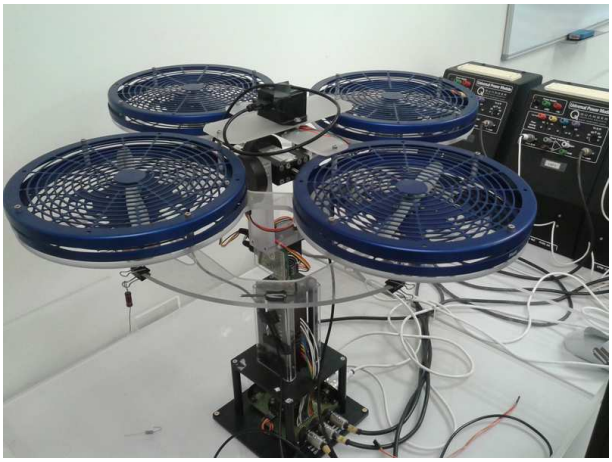

Fig. 1. Experimental platform

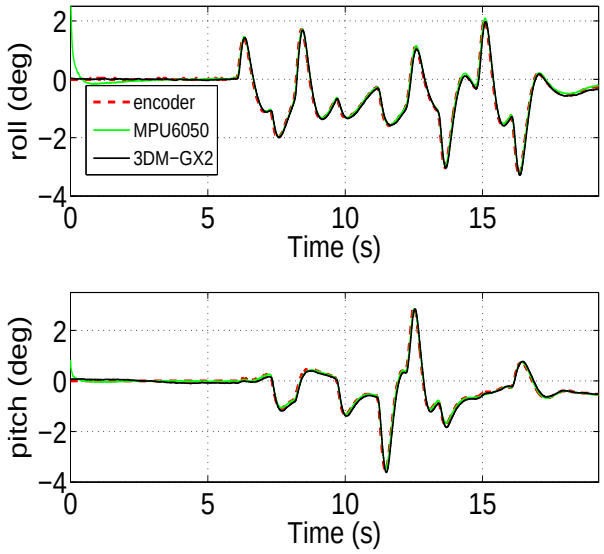

Fig. 2. Attitude estimation

performance indexes were chosen, i.e., the root mean squared error, the maximum absolute error and the delay, all of them computed with respect to the estimation given by the encoders. Table II gathers the information of these indexes for an experiment of several minutes. One can see how the proposed algorithm performs even better than the 3DM-GX2.

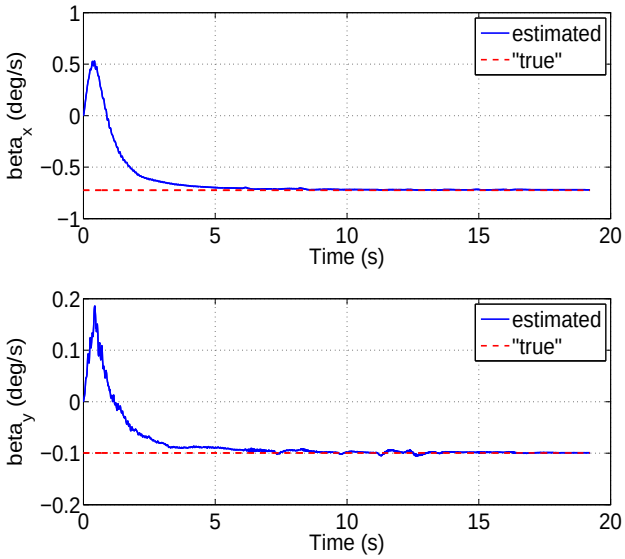

Fig. 3. Bias estimation

Fig. 3 shows the evolution of the bias estimation. The real bias of the gyroscopes was computed averaging the first few seconds during which the system remains steady. It is possible to see how the estimated bias converges to the real

TABLE II

PERFORMANCE INDEXES

		rmse	$\|\text{error}\|_{\max}$	delay
3DM-GX2	roll	0.3 deg	1.56 deg	25 ms
	pitch	0.27 deg	1.46 deg	
MPU 6050	roll	0.14 deg	0.72 deg	15 ms
	pitch	0.19 deg	0.91 deg	

value within a few seconds.

The accelerations measured by the MPU6050 are depicted in Fig. 4 along with the ideal measurements, which were built by computing (4) using the angular measurements from the encoders and adding Gaussian noise. It is pointed out that the accelerometers are easily affected by the vibrations of the motors.

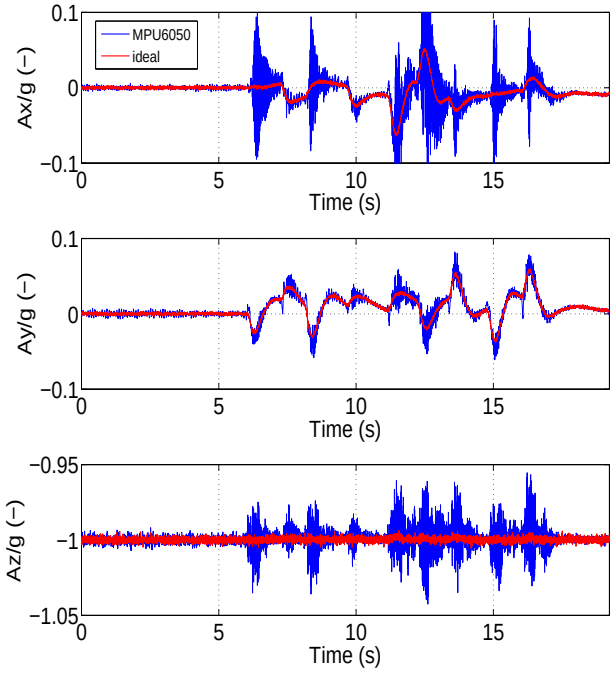

Fig. 4. Accelerometer responses

V. FLIGHT TESTS

Quadrotor prototype

Although the platform described above is a suitable scenario for numerical comparison, there are two handicaps to overcome in real flight, i.e., vibrations and linear accelerations. The proposed algorithm has been also validated in-flight using a small quadrotor specially built for this task, see Fig. 5. It has a distance of 41 cm between rotors, it weights around 1.3 kg without battery, and it is outfitted with an IMU MicroStrain 3DM-GX2 and with the MPU6050, among other sensors.

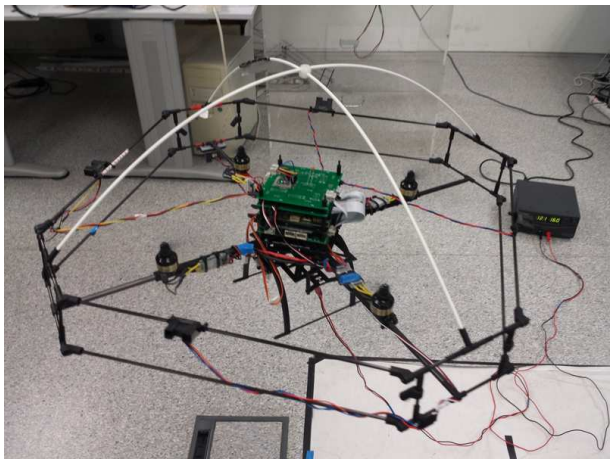

Fig. 5. Quadrotor prototype

The basic hardware consists of a MikroKopter frame, YGE 25i electronic speed controllers, RobbeRoxxy 2827-35 brushless motors and 10x4.5 plastic propellers. All the computations are made onboard using an Arduino Due which is based on an Atmel SAM3X8E ARM Cortex-M3 microcontroller running at 84 MHz, and an Igep v2 board running Xenomai real-time operating system at 1 GHz. .

The Arduino Due is in charge of reading every sensor, running the Kalman filter algorithm for attitude estimation and the attitude control algorithm, controlling the motor's speed, and sending the data to the Igep board. The control algorithm consists of a PD controller with nested saturations. So far the Igep board is only used as Wifi bridge.

Although the proposed algorithm itself takes only 2 milliseconds to run, the main loop in the microcontroller runs at 333 Hz restricted by the communications with the 3DM-GX2 and the Igep board.

Experiments

The quadrotor was controlled in roll and pitch angles using the estimated values, $\hat{\phi}, \hat{\theta}$ and $\hat{\dot{\phi}}, \hat{\dot{\theta}}$, computed using the proposed algorithm. The yaw angle was stabilized with the measurement of the Microstrain sensor.

In the lack of a motion capture system, the in-flight attitude estimation of the proposed algorithm is compared to the 3DM-GX2. Fig. 6 shows the attitude estimation during one minute of flight. One can see that both estimations are very similar. Although the 3DM-GX2 is not a fully reliable pattern, it can be seen that the proposed algorithm provides a fast, noise-free and drift-free estimation. Furthermore, it must be also noticed that the control is computed with the attitude estimation of the proposed algorithm. The small oscillations around the equilibrium point evidence that the attitude and velocity estimations lead to a very good control performance.

The angular velocities are shown in Fig. 7. The estimated angular velocities consist of the raw gyroscope measurements

corrected with the estimated biases. The estimation of the bias avoids the need of correcting the offset of the gyroscopes prior to each flight and allows operation over long periods of time.

VI. Conclusion

A simplified algorithm for attitude estimation based on the Kalman filter has been proposed and validated in-flight. The simplifications in both the dynamic and measurement models result in a very computationally-efficient algorithm.

Despite the simplifications, a comparison carried out in an experimental platform with a reliable pattern provided by optical encoders showed that the proposed algorithm exhibits even better performance than a commercial IMU, the Microstrain 3DM-GX2. Further validation in-flight showed that the proposed algorithm performs also very well under strong vibrations and linear accelerations.

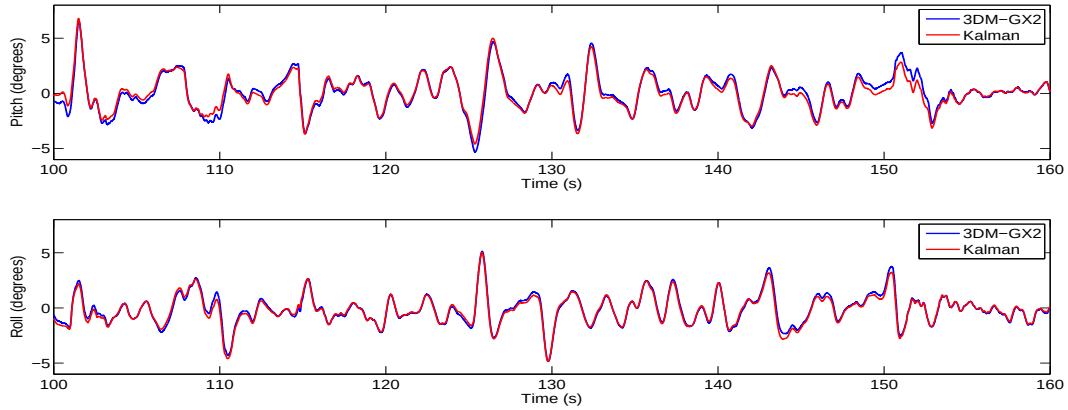

Fig. 6. Comparison of the attitude estimations in-flight

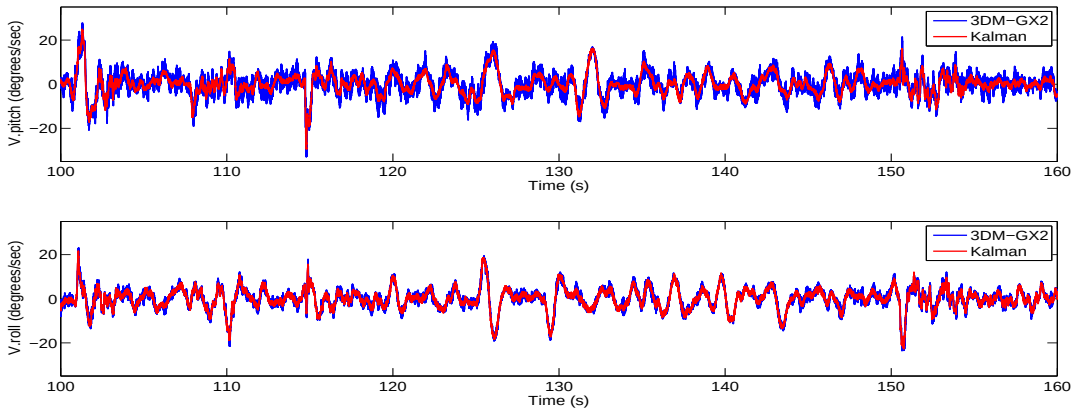

Fig. 7. Comparison of the angular velocity estimations in-flight.

REFERENCES

[1] L. Mejias, J. F. Correa, I. Mondragón, and P. Campoy, "Colibri: a vision-guided uav for surveillance and visual inspection," in *Robotics and Automation, 2007 IEEE International Conference on*. IEEE, 2007, pp. 2760–2761.

[2] D. W. Casbeer, R. Beard, T. McLain, S.-M. Li, and R. K. Mehra, "Forest fire monitoring with multiple small uavs," in *American Control Conference, 2005. Proceedings of the 2005*. IEEE, 2005, pp. 3530–3535.

[3] H. Chao, M. Baumann, A. Jensen, Y. Chen, Y. Cao, W. Ren, and M. McKee, "Band-reconfigurable multi-uav-based cooperative remote sensing for real-time water management and distributed irrigation control," in *IFAC World Congress, Seoul, Korea*, 2008.

[4] "Unmanned systems integrated roadmap," in *FY2013-2038*, 2013.

[5] H. Chao, Y. Cao, and Y. Chen, "Autopilots for small unmanned aerial vehicles: a survey," *International Journal of Control, Automation and Systems*, vol. 8, no. 1, pp. 36–44, 2010.

[6] J. L. Crassidis, F. L. Markley, and Y. Cheng, "Survey of nonlinear attitude estimation methods," *Journal of Guidance, Control, and Dynamics*, vol. 30, no. 1, pp. 12–28, 2007.

[7] J. L. Farrell, "Attitude determination by kalman filtering," *Automatica*, vol. 6, no. 3, pp. 419–430, 1970.

[8] E. J. Lefferts, F. L. Markley, and M. D. Shuster, "Kalman filtering for spacecraft attitude estimation," *Journal of Guidance, Control, and Dynamics*, vol. 5, no. 5, pp. 417–429, 1982.

[9] J. L. Crassidis and F. L. Markley, "Predictive filtering for nonlinear systems," *Journal of Guidance, Control, and Dynamics*, vol. 20, no. 3, pp. 566–572, 1997.

[10] ——, "Unscented filtering for spacecraft attitude estimation," *Journal of guidance, control, and dynamics*, vol. 26, no. 4, pp. 536–542, 2003.

[11] F. L. Markley, J. L. Crassidis, and Y. Cheng, "Nonlinear attitude filtering methods," in *AIAA Guidance, Navigation, and Control Conference*, 2005.

[12] O. Magnussen, M. Ottestad, and G. Hovland, "Experimental validation of a quaternion-based attitude estimation with direct input to a quadcopter control system," in *Unmanned Aircraft Systems (ICUAS), 2013 International Conference on*. IEEE, 2013, pp. 480–485.

[13] P. Martin and E. Salaun, "The true role of accelerometer feedback in quadrotor control," in *Robotics and Automation (ICRA), 2010 IEEE International Conference on*. IEEE, 2010, pp. 1623–1629.

[14] J. L. Crassidis and J. L. Junkins, *Optimal estimation of dynamic systems*. CRC press, 2011.